(101)-Exposed Anatase TiO_2 Nanosheets

Chih-Wei Peng,[†,‡] Tsung-Yin Ke,[§] Luc Brohan,*[,‡] Mireille Richard-Plouet,[‡] Ju-Chun Huang,[§] Eric Puzenat,[||] Hsin-Tien Chiu,[†] and Chi-Young Lee*[,§]

Department of Applied Chemistry, National Chiao Tung University, Taiwan 30050, R.O.C., Department of Materials Science and Engineering and Center for Nanotechnology, Materials Science and Microsystems, National Tsing Hua University, Taiwan 30043, R.O.C., Institut des Matériaux Jean Rouxel (IMN), UMR 6502, 44322 Nantes, France, and Laboratoire d'Application de la Chimie à l'Environnement, UMR 5634, CNRS-Université Claude Bernard Lyon 1, 69622 Villeurbanne, France

Received April 16, 2007
Revised Manuscript Received January 27, 2008

As a result of a wide range of potential applications, photochemistry of titanium dioxide (TiO_2) is a fast growing area.[1,2] With specific nanostructural control of morphology, the performance of TiO_2 can be optimized. A recent report by Selloni and Diebold suggests that anatase TiO_2 with exposed step edges on the (101) surface may show high active site density and enhanced photocatalytic activity.[3] Lately, titanate nanotubes,[4–6] nanowires,[7] and nanosheets[5] have been synthesized via chimie-douce (soft chemistry) routes, performed under atmospheric and autogenous (sealed autoclave) pressures at low temperatures. These titanates can be easily converted into TiO_2 with special morphologies by appropriate ion-exchange treatments.[8] Although a flower-like titanate nanosheet has been observed in several works,[5,9,10] it is frequently regarded as a byproduct or an intermediate in the formation process of titanate nanotubes. Therefore, it has never been well isolated and characterized. Its conversion into TiO_2 and investigation of its photoactivity have not been reported either. In this work, we demonstrate for the first time how to prepare an anatase TiO_2 nanosheet with active sites, along (101) planes of anatase by a chimie-douce method. Indeed, this material exhibits excellent photocatalytic activity.

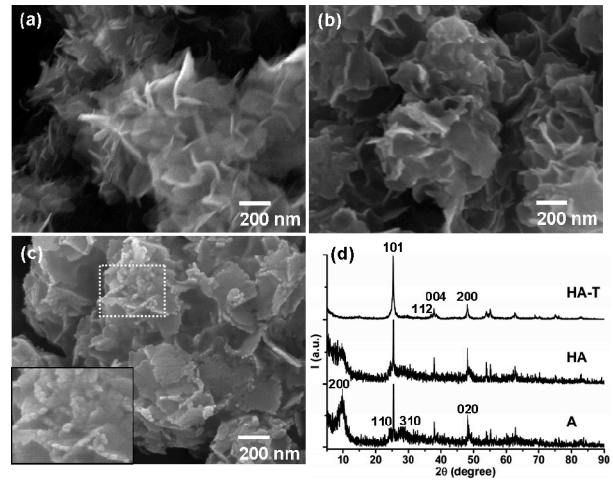

Figure 1. SEM images of flower-like titanate nanosheets (a) **A**, (b) **HA**, and (c) **HA-T**; (d) XRD patterns of **A**, **HA**, and **HA-T**.

Commercial anatase TiO_2 powder suspended in 15 M NaOH(aq) was refluxed in air atmosphere at 423 K for 24–72 h. The isolated solid was rinsed with deionized water and dried at 343 K to give product **A**. When 10 M NaOH(aq) was applied to an analogous reaction process, product **B** can be obtained. **A** was immersed in 0.1 M HNO_3(aq), rinsed with deionized water, and dried at 343 K under air to produce an H^+ exchanged product, **HA**. **HB** can be obtained from **B** using the same treatment. Heating **HA** and **HB** at 623 K in air atmosphere for 4 h produced solid phases **HA-T** and **HB-T**, respectively.

Scanning electron microscopy (SEM) micrographs in Figure 1a−c exhibit the morphology of **A**, **HA**, and **HA-T**, respectively. **A** is composed of uniform nanosheets with width 100–300 nm and thickness less than 10 nm. After H^+-exchange and post-heat-treatment, **HA** and **HA-T** retained the overall sheet-like morphology and dimension of **A**. Close examination of the images suggests that the layer edges of **HA** shrank slightly while those of **HA-T** roughened into an apparent assembly of small particles. Brunauer–Emmett–Teller (BET) experiments show specific areas of **A**, **HA**, and **HA-T** to be 224, 200, and 278 $m^2\ g^{-1}$, respectively. They are much higher than the specific area of Degussa P25, 50 $m^2\ g^{-1}$. For **HA-T**, the increased specific area agrees well with the apparent increase of roughness observed in SEM. On the other hand, **B** and **HB** consisted of nanotubes formed by rolling up of titanate nanolayers, with an average 8 nm outer diameter, 2.4 nm thick wall, and length 20–500 nm. These findings agree well with literature reports.[6,11] The morphology of **HB-T** changed to particle aggregates and rod-like shapes with diameter approximately 8 nm and length 10–200 nm. Specific areas of **B**, **HB**, and **HB-T** are 262, 284, and 323 $m^2\ g^{-1}$, respectively. Apparently, the heat-treatment process altered the physical shape of **HB-T** significantly. The length-to-width (average tube or rod

[†] National Chiao Tung University.
[‡] Institut des Matériaux Jean Rouxel (IMN).
[§] National Tsing Hua University.
[||] CNRS-Université Claude Bernard Lyon 1.

(1) Mills, A.; Lee, S.-K. *J. Photochem. Photobiol., A* **2002**, *152*, 233.
(2) Carp, O.; Huisman, C. L.; Reller, A. *Prog. Solid State Chem.* **2004**, *32*, 33.
(3) (a) Vittadini, A.; Selloni, A.; Rotzinger, F. P.; Grätzel, M. *Phys. Rev. Lett.* **1998**, *81*, 2954. (b) Gong, X.-Q.; Selloni, A. *J. Phys. Chem. B* **2005**, *109*, 19560. (c) Gong, X.-Q.; Selloni, A.; Batzill, M.; Diebold, U. *Nat. Mater.* **2006**, *5*, 665.
(4) Kasuga, T.; Hiramatsu, M.; Hoson, A.; Sekino, T.; Niihara, K. *Adv. Mater.* **1999**, *11*, 1307.
(5) Chen, Y.-F.; Lee, C.-Y.; Yeng, M.-Y.; Chiu, H.-T. *Mater. Chem. Phys.* **2003**, *81*, 39.
(6) Chen, Q.; Zhou, W.; Du, G.; Peng, L.-M. *Adv. Mater.* **2002**, *14*, 1208.
(7) Armstrong, A. R.; Armstrong, G.; Canales, J.; Bruce, P. G. *Angew. Chem., Int. Ed.* **2004**, *43*, 2286.
(8) Yoshida, R.; Suzuki, Y.; Yoshikawa, S. *J. Solid State Chem.* **2005**, *178*, 2179.
(9) Matsuda, A.; Matoda, T.; Kogure, T.; Tadanaga, K.; Minami, T.; Tatsumisago, M. *Chem. Mater.* **2005**, *17*, 749.
(10) Takezawa, Y.; Imai, H. *Small* **2006**, *2*, 390.
(11) Tsai, C.-C.; Teng, H. *Chem. Mater.* **2004**, *16*, 4352.

10.1021/cm071038e CCC: $40.75
Published on Web 03/07/2008

diameter) aspect ratio decreased from a range of 2.5–62.5 to 1.25–25 for **HB** and **HB-T**, respectively.

The X-ray diffraction (XRD) patterns in Figure 1d reveal that **A** and **HA** have similar lattice parameters. They can be assigned to a lepidocrocite type (JCPDS 47-0124) structure. In addition, sharp peaks from residual anatase TiO_2 are observed for both samples. The peaks of **HA** became broader than those of **A**, indicating that **HA** is less ordered than **A**. Through dehydration of **HA** at 623 K, it completely transforms back to the anatase phase TiO_2 **HA-T**, as shown in Figure 1d. **HA-T** shows an intensity ratio of (101) and (112) reflections, $I_{(101)}/I_{(112)}$, that is twice as intense as the expected value of a randomly oriented anatase (JCPDS 21-1272). This implies that **HA-T** has a preferred growth in the [101] direction which exposes more (101) planes than the randomly oriented anatase. The layered morphology of **HA-T** agrees with this. Reflections from a trace amount of TiO_2(B) can be observed in **HA-T**.[7] For comparison, **B** and **HB** nanotubes also showed patterns assignable to lepidocrocite-type structures.[11,12] After dehydration of **HB**, **HB-T** contained mainly anatase phase while some TiO_2(B) was formed also.[7] This material did not crystallize as well as **HA-T**, and its (101) reflection was not as intense as that of the heat-treated nanosheet.

We used energy dispersive X-ray (EDX) spectroscopy and thermogravimetric analysis coupled to mass spectroscopy (TGA/MS) to study the chemical composition of the as-prepared samples. From EDX results, we knew that the Na/Ti ratios were close to 0.4 for both **A** and **B**. After the H^+ exchange steps, we did not observe any Na in **HA** and **HB**. Using the TGA/MS data, we estimated that the H_2O/titanate ratios are 0.9, 0.8, 0.6, and 0.5 for **A**, **B**, **HA**, and **HB**, respectively. Residual anatase TiO_2 in **A** and **HA** were expected to be negligible in this estimation. Thus, we are able to express the empirical formulas of **A**, **B**, **HA**, and **HB** to be "$Na_{0.8}H_{1.2}Ti_2O_5 \cdot 1.2H_2O \cdot 0.02CO_2$", "$Na_{0.8}H_{1.2}Ti_2O_5 \cdot H_2O$", "$H_2Ti_2O_5 \cdot 0.2H_2O \cdot 0.02CO_2$", and "$H_2Ti_2O_5$", respectively.

Transmission electron microscopy (TEM) images shown in Figure 2 reveal that dimensions of the nanosheets **A**, **HA**, and **HA-T** are well in agreement with the data found in the SEM observations. From fringes shown in a high-resolution TEM (HRTEM) image of **A** in Figure 2b, the interlayer distance is identified to be 0.89 nm. This value agrees with the spacing of the (200) planes of a lepidocrocite type structure, which is also observed in the XRD result. In Figure 2c, an HRTEM image of the surface of a nanosheet **A** exhibited a noncorrugated layer structure. Figure 2d is a Fourier transformed (FT) pattern from the selected area in Figure 2c. It matched well with the calculated electron diffraction pattern viewing along [133] of a lepidocrocite-type structure. The filtered image from Fourier transformation of Figure 2d showed only one pair of fringes with distance 0.28 nm × 0.34 nm, as shown in Figure 2e. There are no large distance fringes originated from a stepped layer or a tunnel titanate structure. The TEM images of **HA**, shown in Figure 2f,g, are similar to those of **A**, but the displayed interlayer distance is lower and close to 0.65 nm. This does not match the (200) peak position observed for **HA** in the XRD (Figure 1d). The shrinkage may have resulted from the escape of interlayer water molecules from the lattice of **HA** in the ultrahigh vacuum of the TEM chamber. In the TEM image of **HA-T** shown in Figure 3a, sheets appear to be divided into different orientation domains while retaining the initial sheet morphology (Figure 1c). These were probably generated during the dehydration−condensation process that shrank the crystallites of **HA**. The HRTEM of **HA-T** in Figure 3 shows that the nanosheet is assembled from many connected small crystallites with sizes 1–10 nm. The image

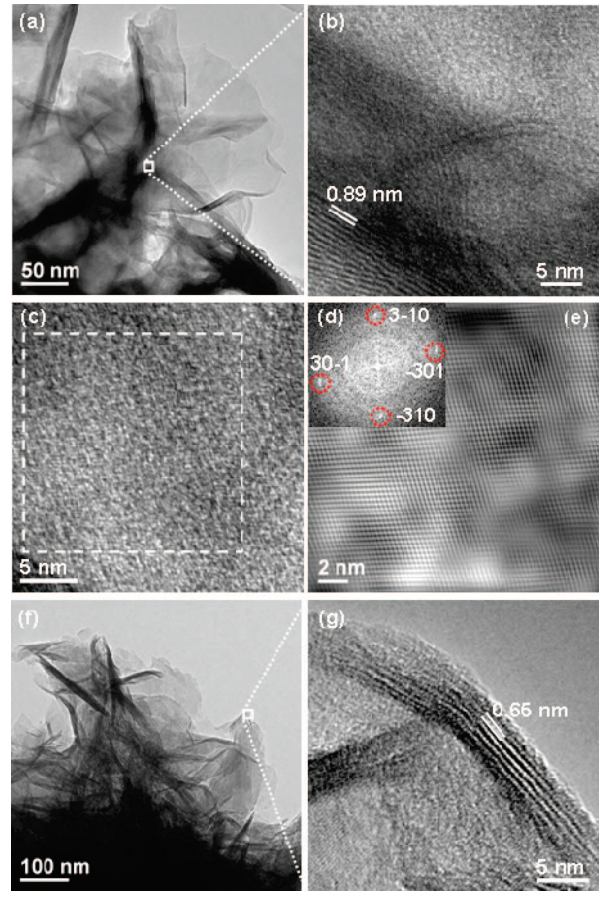

Figure 2. (a) TEM and (b) HRTEM images of **A**; (c) HRTEM image of **A**; (d) FT pattern of the white square area selected from (c); (e) inverted FT pattern from (d) viewing along [133] of the lepidocrocite-type structure; and (f) TEM and (g) HRTEM images of **HA**.

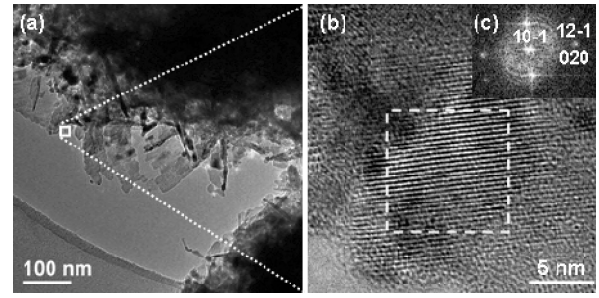

Figure 3. (a) TEM and (b) HRTEM images of **HA-T**; (c) FFT pattern from the white square area selected from (b).

(12) Ma, R.; Bando, Y.; Sasaki, T. *Chem. Phys. Lett.* **2003**, *380*, 577.

Scheme 1. Proposed Pathway To Convert Bulk Anatase to (101) Plane Exposed Nano-Anatase TiO_2 via a Chimie-douce Route[a]

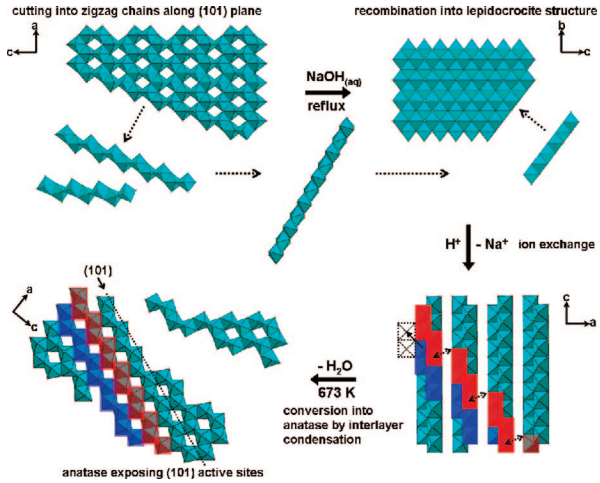

[a] The highlighted red and blue parts are the stepped frame of (101) surface.

shows uneven contrast among crystallites, suggesting that the crystal thickness varies from one area to another. By FT of a selected area of high resolution image in Figure 3b, it was discovered that the simulated diffraction pattern agrees with that of an anatase TiO_2 viewing along the [101]* direction, as shown in Figure 3c. This suggests that the nanocrystallite provides an apparent preferred [101] growth direction. Since the surface of the nanosheet cannot be planar, we propose that a high amount of (101) active sites, such as terraces, steps, and kinks, should exist and be highly exposed in **HA-T**. In photoinduced processes, these sites are regarded as the more active ones among the surfaces of TiO_2 anatase.[3]

To interpret how the (101)-exposed anatase TiO_2 formed, an illustration is proposed in Scheme 1. It suggests a pathway to convert bulk anatase into (101)-exposed anatase TiO_2 nanosheets via a chimie-douce route. In the first step, the initial common anatase is dissolved by concentrated NaOH(aq) into building blocks of zigzag titanate chains.[13] Then, these building blocks crystallize into layered titanates with a lepidocrocite structure. After the Na^+ ions are replaced by H^+ ions, we propose that the final dehydration−condensation involves a topotactic process that not only removes H_2O molecules during the condensation process but also reconstructs the layers. By migrating and connecting the stepped units in the same color, as shown in the last step in the scheme, the (101) site-exposed surface appears. Since **HA** grew as thin nanosheets, the process may also generate **HA-T** with a preferred orientation in [101] direction as the titanate layers of **HA** underwent condensation. This condensation process may also shrink the overall surface of **HA**. This provides a reason to rationalize how the small domains in **HA-T** sheets were generated. In contrast, (101)-exposed anatase could not be produced in the analogous topotactic process to generate **HB-T** from **B**. This is probably due to the highly strained reel structure of **B** and **HB**.

By studying the effect on the photodecomposition of an aqueous solution of methylene blue (25 ppm) under a Xe

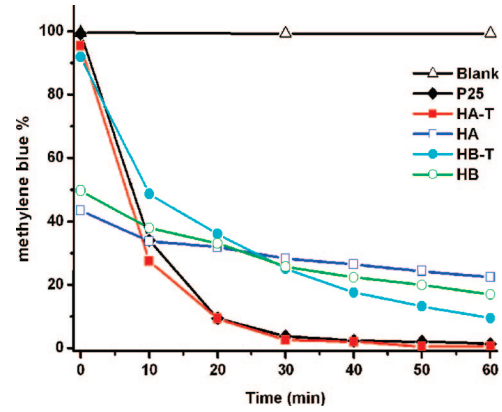

Figure 4. Photocatalytic properties of Degussa P25 TiO_2, **HA**, **HA-T**, **HB**, and **HB-T**. The blank was performed without adding any TiO_2. The concentration decrease in the **HA** and **HB** was due to adsorption. The adsorptions of methylene blue on 1 g of P25, **HA-T**, **HB-T, HB**, and **HA** were 0.5, 2, 4, 25, and 28 mg, respectively.

lamp (Osram 180 W) radiation, the photocatalytic activities of Degussa P25 TiO_2 powder, **HA**, **HA-T**, **HB**, and **HB-T** were compared. As shown in Figure 4, we discover that all four products are photoactive. The initial photocatalytic decomposition rates, r_0, of methylene blue in the presence of **HA-T**, **HA**, **HB-T**, **HB**, P25, and blank (without any TiO_2 added) are 1.7, 0.2, 1.4, 0.3, 1.6, and 0 ppm·min^{-1}, respectively. Among them, **HA-T** shows excellent photocatalytic efficiency, even better than Degussa P25 which is the reported most photoactive of the commercial TiO_2 nanoparticles. From r_0, the photodecomposition efficiency can be ranked in descending order as **HA-T** > Degussa P25 ≫ **HB-T** ≫ **HB** > **HA**. It is interesting to note that even though **HB-T** has a higher specific area, 300 m^2 g^{-1}, than **HA-T**, 278 m^2 g^{-1}, **HA-T** exhibits much higher photocatalytic activity than **HB-T**. This can be explained by the unusually large amount of photoactive (101) sites that **HA-T** exposes. Even though there are reports about good photocatalytic activities of titanic acids,[14] **HA** and **HB** do not perform well as the anatase materials in this study.

In conclusion, the soft chemistry route in the acido−basic approach allows us to control the size and shape of titanate crystallites. By coupling the chimie-douce and heat treatment methods, we have successfully synthesized anatase titanium dioxide nanosheets with highly exposed (101) sites. The material found in this study displays greatly enhanced photocatalytic activity, which provides a strong support to the fundamental studies reported in literature.[3]

Acknowledgment. We thank the NSC and the Ministry of Education of Taiwan, the Republic of China, and CNRS, France, for financial support. We also thank Jacquline Kao for English correction.

Supporting Information Available: The experimental section, TEM images of **B**, HRTEM image of **HA-T**, and TGA/MS results (PDF). This material is available free of charge via the Internet at http://pubs.acs.org.

CM071038E

(13) Peng, C.-W. Joint Thesis of Ph.D., Université de Nantes and National Chiao Tung University, 2006.

(14) Song, Z. Q.; Xu, H. Y.; Li, K. W.; Wang, H.; Yan, H. *J. Mol. Catal. A: Chem.* **2005**, *239*, 87.